

Alignment of the NLO side groups in the layers was achieved by single-point corona poling, with the point source held at +10 kV, at a distance of 1.5 cm from the surface. Poling voltages greater than 10 kV sometimes resulted in damage to the film, manifested as a slight cloudiness. Note, however, that this voltage was still below the saturation point of the signal. The variation of the signal with poling voltages will be discussed more fully in a later publication. Due to the low glass transition temperature of 1 ( $T_g = 25^\circ\text{C}$ ), the poling was carried out at room temperature while the SHG measurements were being made. Upon removal of the voltage, the second-harmonic signal decayed to zero within a few minutes.

The second-harmonic coefficient of the polymer film,  $d_{33}$ , was obtained from a Maker fringe analysis of the data,<sup>10</sup> giving  $d_{33} = 5.5 \text{ pm/V}$ . This value of  $d_{33}$  was obtained by using the isotropic model for poled polymers, where  $d_{33}/d_{31} = 3$ .<sup>2a</sup> Singer et al.<sup>3d</sup> have found this model to be appropriate for analysis of their side-chain polymers. Recently, however, Eich et al.<sup>3e</sup> have observed deviations from this ratio, possible due to mesogenic interactions among the side groups. The applicability of the isotropic model to poly(organophosphazenes) is currently under investigation.

Given that the degree of alignment was not maximized in this experiment and that we are using a less efficient donor moiety than other studies of functionalized polymers,<sup>2c,3d</sup> this is a very promising value of  $d_{33}$ . Work to attach more efficient donors and to increase the glass transition temperature of the polymer is in progress.

**Acknowledgment.** The research at The Pennsylvania State University was supported by the U.S. Air Force Office of Scientific Research and the Office of Naval Research. The research at University of Southern California was supported by the U.S. Air Force Office of Scientific Research. We thank Y. Shi for the refractive index measurements.

(10) Jerphanon, J.; Kurtz, S. K. *J. Appl. Phys.* 1970, 41, 1667.

## Molten Salt Synthesis of Low-Dimensional Ternary Chalcogenides. Novel Structure Types in the K/Hg/Q System (Q = S, Se)

Mercouri G. Kanatzidis\* and Younbong Park

Department of Chemistry and  
Center for Fundamental Materials Research  
Michigan State University  
East Lansing, Michigan 48824

Received December 8, 1989

Recently we demonstrated that by using alkali-metal polysulfide melts as solvents at intermediate temperatures (i.e., 150–350 °C), novel, low-dimensional solid-state compounds can be isolated in crystalline form.<sup>1</sup> This intermediate temperature regime has not been explored as a synthetically useful area.<sup>2</sup> It has been regarded by mo-

(1) Kanatzidis, M. G.; Park, Y. *J. Am. Chem. Soc.* 1989, 111, 3767–3769.

(2) This does not include the hydrothermal synthesis technique which also involves solvents in high pressures (supercritical state). However, chalcogenide synthesis under these conditions is also a relatively unexplored area. For examples of such synthesis, see: (a) Sheldrick, W. S. *Z. Anorg. Allg. Chem.* 1988, 562, 23–30. (b) Sheldrick, W. S.; Hauser, H.-J. *Z. Anorg. Allg. Chem.* 1988, 557, 98–104. (c) Sheldrick, W. S.; Hauser, H.-J. *Z. Anorg. Allg. Chem.* 1988, 557, 105–111.

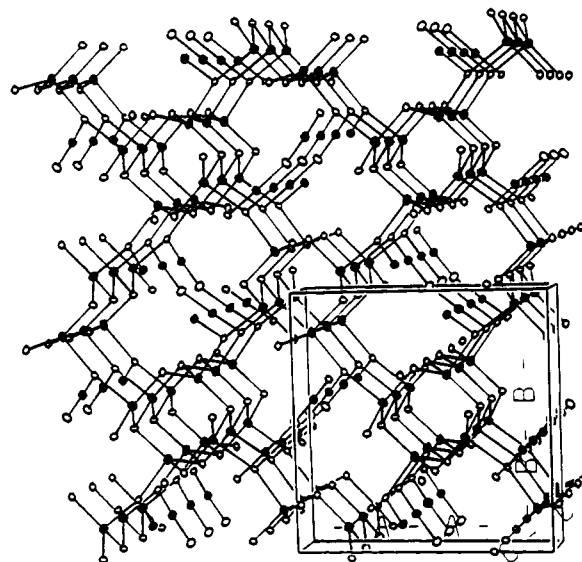


**Figure 1.** Three-dimensional structure of the  $[\text{Hg}_6\text{S}_7]^{2n-}$  network.<sup>17,18</sup> The K atoms have been omitted for clarity. The Hg atoms are represented by black circles and the sulfur atoms by open circles. The S–Hg–S angle about the two-coordinate Hg atom is  $172.4(4)^\circ$ .

lecular coordination chemists as too hot for any normal solvents to be stable and stay in liquid form and by classical solid-state chemists as too cold for most reactions to proceed. This is particularly true in chalcogenide chemistry.<sup>3</sup> We believe that an enormous number of interesting and perhaps metastable compounds occur at these temperatures and could be crystallized, provided suitable solvents are available. Molten salts have been well studied<sup>4</sup> and can be prepared to exhibit a wide range of temperatures at which they remain liquid and thus are appropriate media for synthetic applications. Indeed they have been used as such at high temperatures.<sup>5</sup> Alkali-metal polychalcogenide melts in particular are very interesting because melting points as low as  $\sim 150^\circ\text{C}$  can be achieved<sup>6</sup> and can serve as solvents as well as reagents (i.e., chalcogen and alkali-metal donors). Recrystallizations of binary sulfides have been accomplished in these melts at high ( $>700^\circ\text{C}$ ) temperatures.<sup>7</sup> The purposeful use of these systems for synthesis of new materials has not been seriously pursued. Low-dimensional chalcogenides are of intense interest due to their useful electronic<sup>8</sup> and catalytic<sup>9</sup>

(3) (a) Roberts, L. E. *J. MTP Int. Rev. Sci., Inorg. Chem.* 1972, 10, 189–241. (b) Bronger, W. *Angew. Chem., Int. Ed. Engl.* 1981, 20, 52–62. (c) Meerschaut, A.; Gressier, P.; Guemas, L.; Rouxel, J. *J. Solid State Chem.* 1984, 51, 307–314.

(4) (a) *Ionic Liquids*: Inman, D., Lovering D. J., Eds.; Plenum Press: New York, 1981. (b) Feigelson, R. S. *Adv. Chem. Ser.* 1980, 186, 243–275. (c) Wold, A.; Bellavance, D. In *Preparative Methods in Solid State Chemistry*; Hagemmuller, P., Ed.; Academic Press: New York, 1972; pp 279–308.

(5) (a) Elwell, D.; Scheel, H. J. In *Crystal Growth from High-Temperature Solutions*; Academic Press: London, 1975. (b) *Molten Salts Handbook*; Janz, G. J., Ed.; Academic Press: London, 1975. (c) *Molten Salts*; Mamantov, G., Ed.; Marcel Dekker: New York, 1969.

(6) (a) Klemm, W.; Sodomann, H.; Langmesser, P. *Z. Anorg. Allg. Chem.* 1939, 241, 281–304. (b) Pearson, T. G.; Robinson, P. L. *J. Chem. Soc.* 1931, 1304–1314.

(7) (a) Scheel, H. *J. Cryst. Growth* 1974, 24/25, 669–673. (b) Sanjines, R.; Berger, H.; Levy, F. *Mater. Res. Bull.* 1988, 23, 549–553. (c) Garner, R. W.; White, W. B. *J. Cryst. Growth* 1970, 7, 343–347.

(8) (a) Meerschaut, A.; Rouxel, J. In *Crystal Chemistry and Properties of Materials with Quasi One-Dimensional Structures*; Rouxel, J., Ed.; D. Reidel: 1986; pp 205–279. (b) Fischer, O., Maple, M. B., Eds.; *Superconductivity in Ternary Compounds*; Springer: Berlin, 1982; Vols. I and II. (c) Chevrel, R. In *Superconductor Materials Science: Metallurgy, Fabrication and Applications*; Foner, S., Schwartz, B. B., Eds.; Plenum Press: New York, 1981; Chapter 10. (d) Whittingham, M. S. *Prog. Solid State. Chem.* 1978, 12, 41–99.

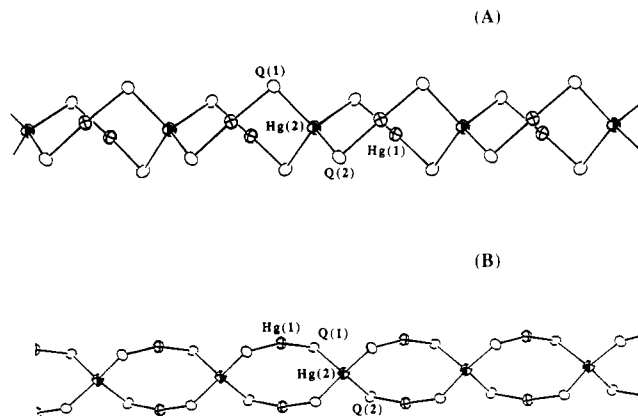
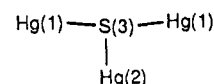


**Figure 2.** Two views of the one-dimensional structure of  $[\text{Hg}_3\text{Q}_4]_n^{2n-}$  with labeling scheme. Selected distances (Å):  $\text{K}_2\text{Hg}_3\text{S}_4$ :  $\text{Hg}(1)\text{-S}(1)$ , 2.36 (1);  $\text{Hg}(1)\text{-S}(2)$ , 2.38 (1);  $\text{Hg}(2)\text{-S}(1)$ , 2.58 (1);  $\text{Hg}(2)\text{-S}(2)$ , 2.56 (1). Selected angles (deg):  $\text{S}(1)\text{-Hg}(1)\text{-S}(2)$ , 165.3 (3);  $\text{S}(1)\text{-Hg}(2)\text{-S}(2)$ , 105.7 (3);  $\text{S}(2)\text{-Hg}(2)\text{-S}(2)$ , 111.0 (4);  $\text{S}(1)\text{-Hg}(2)\text{-S}(1)$ , 104.7 (3);  $\text{S}(1)\text{-Hg}(2)\text{-S}(2)$ , 114.9 (3);  $\text{Hg}(1)\text{-S}(1)\text{-Hg}(2)$ , 96.5 (3);  $\text{Hg}(1)\text{-S}(2)\text{-Hg}(2)$ , 95.8 (3).  $\text{K}_2\text{Hg}_3\text{Se}_4$ :  $\text{Hg}(1)\text{-Se}(1)$ , 2.486 (6);  $\text{Hg}(1)\text{-Se}(2)$ , 2.474 (6);  $\text{Hg}(2)\text{-Se}(1)$ , 2.671 (6);  $\text{Hg}(2)\text{-Se}(2)$ , 2.657 (6).  $\text{Se}(1)\text{-Hg}(1)\text{-Se}(2)$ , 164.2 (2);  $\text{Se}(1)\text{-Hg}(2)\text{-Se}(2)$ , 104.4 (2);  $\text{Se}(2)\text{-Hg}(2)\text{-Se}(2)$ , 110.7 (2);  $\text{Se}(1)\text{-Hg}(2)\text{-Se}(1)$ , 106.2 (2);  $\text{Se}(1)\text{-Hg}(2)\text{-Se}(2)$ , 115.7 (2);  $\text{Hg}(1)\text{-Se}(1)\text{-Hg}(2)$ , 95.7 (2);  $\text{Hg}(1)\text{-Se}(2)\text{-Hg}(2)$ , 95.8 (2).

properties, and therefore new such materials and/or methods of synthesis are highly desirable.<sup>10</sup> Recently the compounds  $\text{K}_4\text{Ti}_3\text{S}_{14}$ ,<sup>11</sup>  $\text{Na}_2\text{Ti}_2\text{Se}_3$ ,<sup>12</sup> and  $\text{K}_3\text{Nb}_2\text{Se}_{11}$ <sup>13</sup> were reported to form in polychalcogenide melts at 340–375 °C. In this report we show that alkali-metal polychalcogenide melts at 210–250 °C promote the synthesis and crystal growth of the new ternary compounds  $\text{K}_2\text{Hg}_6\text{S}_7$  and  $\text{K}_2\text{Hg}_3\text{Q}_4$  (Q = S, Se), which feature novel structure types.

The reaction of 0.348 g (2 mmol) of  $\text{K}_2\text{S}_3$  and 0.100 g (0.50 mmol) of Hg (or HgS) in an evacuated Pyrex tube at 210 °C for 3 days afforded black needle-shaped crystals of  $\text{K}_2\text{Hg}_6\text{S}_7$  (I) in quantitative yield. The product was isolated by removing the excess  $\text{K}_2\text{S}_3$  by water. Alternatively, the reaction of 0.310 g (1.5 mmol) of  $\text{K}_2\text{S}_4$  and 0.116 g (0.5 mmol) of HgS in an evacuated Pyrex tube at 220 °C for 4 days afforded yellow hexagon-shaped, light- and moisture-sensitive  $\text{K}_2\text{Hg}_3\text{S}_4$  (II). This product was isolated under nitrogen atmosphere by dissolving the excess  $\text{K}_2\text{S}_4$  with dimethylformamide. The isomorphous selenium analogue,  $\text{K}_2\text{Hg}_3\text{Se}_4$  (III), was synthesized in an analogous manner at 250 °C.<sup>14</sup> The structures of these materials were established by single-crystal X-ray diffraction studies.<sup>15</sup>

The structure type of  $\text{K}_2\text{Hg}_6\text{S}_7$  is unique. Although the  $\text{Hg}^{2+}$  and  $\text{S}^{2-}$  atoms are assembled in three dimensions, the structure clearly possesses one-dimensional (1-D) character. There are clearly visible 1-D tunnels running through the lattice parallel to the crystallographic  $c$  axis, as shown in Figure 1. Two different sets of parallel tunnels exist. A set of empty, narrow tunnels with an octagonal cross section composed of tetrahedral (distorted)  $\text{Hg}^{2+}$  and trigonal-pyramidal  $\text{S}^{2-}$  ions. The diameter of these narrow tunnels is ca. 4.77 Å. A second set of wider tunnels have 12-membered ring cross section in which both tetrahedral and linear  $\text{Hg}^{2+}$  ions exist and are “glued” together by triply and doubly bridging  $\text{S}^{2-}$  ions. One triply bridging  $\text{S}^{2-}$  ion assumes a T-type coordination as shown here: The



$\text{Hg}(1)\text{-S}(3)\text{-Hg}(1)$  and  $\text{Hg}(1)\text{-S}(3)\text{-Hg}(2)$  angles are 158.1° and 100.9°, respectively. The coordination of the  $\text{Hg}(1)$  atoms is tetrahedral while that of the  $\text{Hg}(2)$  atoms is linear. The  $\text{Hg}(1)\text{-S}(3)$  bonds are unusually long at 2.718 (4) Å, while the  $\text{Hg}(2)\text{-S}(3)$  bonds are normal (for two-coordinate  $\text{Hg}^{2+}$  ion) at 2.345 (8) Å.

The  $\text{K}^+$  ions are found inserted in the center of the large tunnels, interacting with the chalcogenide lone pairs which are directed toward the tunnel center. This structure type is reminiscent of a 3-D zeolite-like network.<sup>16</sup> The  $\text{K}\cdots\text{S}$  distances are found in the range 3.299–3.618 Å. There are two kinds of Hg–S bonds in  $\text{K}_2\text{Hg}_6\text{S}_7$ . A set of long bonds (range 2.467 (5)–2.718 (5) Å) is associated with the tetrahedral  $\text{Hg}^{2+}$  centers, and a set of short ones (range 2.345 (8)–2.366 (9) Å) associated with the linear  $\text{Hg}^{2+}$  centers.<sup>17,18</sup>

The structure of  $\text{K}_2\text{Hg}_3\text{Q}_4$  is shown in Figure 2. It is composed of centrosymmetric one-dimensional  $[\text{Hg}_3\text{Q}_4]_n^{2n-}$  chains running parallel to the  $b$  axis. The makeup of the chains can be regarded as a one-dimensional assembly of distorted tetrahedral  $[\text{HgQ}_4]^{6-}$  building blocks connected by two-coordinate  $\text{Hg}^{2+}$  ions. Alternatively it can be viewed as a one-dimensional spiropolymer of eight-membered  $\text{Hg}_4\text{Q}_4$  rings. As in  $\text{K}_2\text{Hg}_6\text{S}_7$ , there are two sets of long and short Hg–Q bonds in this structure type, associated with tetrahedral and quasi-linear  $\text{Hg}^{2+}$  centers, respectively. Selected bond distances for  $\text{K}_2\text{Hg}_3\text{Se}_4$  are given in the caption of Figure 2.

The compounds  $\text{K}_2\text{Hg}_3\text{Se}_4$  and  $\text{K}_2\text{Hg}_3\text{S}_4$  decompose rapidly in moist air and light to form black HgQ. Both types of compounds,  $\text{K}_2\text{Hg}_3\text{Q}_4$  and  $\text{K}_2\text{Hg}_6\text{S}_7$ , can be regarded as members of a new general family with the chemical formula  $(\text{A}_2\text{Q})_n(\text{HgQ})_m$  (A = alkali metal). Their

(9) (a) Alonso Vante, N.; Jaegermann, W.; Tributsch, H.; Hönle, W.; Yvon, K. *J. Am. Chem. Soc.* **1987**, *111*, 3251–3257. (b) Weisser, O.; Landa, S. *Sulfide Catalysis: Their Properties and Applications*; Pergamon: London, 1973. (c) Chianelli, R. R.; Pecoraro, T. A.; Halbert, T. R.; Pan, W.-H.; Stiefel, E. I. *J. Catal.* **1984**, *86*, 226–230. (d) Pecoraro, T. A.; Chianelli, R. R. *J. Catal.* **1981**, *67*, 430–445.

(10) (a) Rouxel, J. In *Crystal Chemistry and Properties of Materials with Quasi One-Dimensional Structures*; Rouxel, J., Ed.; D. Reidel: 1986; pp 1–26. (b) Sunshine, S. A.; Keszler, D. A.; Ibers, J. A. *Acc. Chem. Res.* **1987**, *20*, 395–400. (c) Rouxel, J. *Mol. Cryst. Liq. Cryst.* **1985**, *121*, 1–13. (d) Keszler, D. A.; Ibers, J. A. *J. Am. Chem. Soc.* **1985**, *107*, 8119–8127. (e) Gressier, P.; Meerschaut, A.; Guemas, L.; Rouxel, J.; Monceau, P. *J. Solid State Chem.* **1984**, *51*, 141–151.

(11) Sunshine, S. A.; Kang, D.; Ibers, J. A. *J. Am. Chem. Soc.* **1987**, *109*, 6202–6204.

(12) Kang, D.; Ibers, J. A. *Inorg. Chem.* **1988**, *27*, 549–551.

(13) Schreiner, S.; Aleandri, L. E.; Kang, D.; Ibers, J. A. *Inorg. Chem.* **1989**, *28*, 392–393.

(14) The analogous  $\text{K}_2\text{Hg}_6\text{Se}_7$  could not be prepared probably because  $\text{K}^+$  is too small to support the enlarged tunnels in this structure. Experiments are under way to determine whether this structure can be stabilized with larger alkali-metal ions such as  $\text{Rb}^+$  and  $\text{Cs}^+$ .

(15) (a) Crystal data for  $\text{K}_2\text{Hg}_6\text{S}_7$ : tetragonal  $P4_2/m$   $Z = 2$ ,  $a = b = 13.805$  (8) Å,  $c = 4.080$  (3) Å,  $V = 778$  Å<sup>3</sup> at 25 °C.  $2\theta_{\text{max}}(\text{MoK}\alpha) = 50^\circ$ . Number of data measured, 1614. Number of unique data, 453. Number of data having  $F_o^2 > 3\sigma(F_o^2)$ , 402. Number of variables, 42. Number of atoms, 6.  $\mu = 604$  cm<sup>-1</sup>. Final  $R = 0.031$  and  $R_w = 0.036$ . (b) Crystal data for  $\text{K}_2\text{Hg}_3\text{S}_4$ : orthorhombic  $Pbcn$ ,  $Z = 4$ ,  $a = 10.561$  (5) Å,  $b = 6.534$  (3) Å,  $c = 13.706$  (2) Å,  $V = 946$  Å<sup>3</sup> at 25 °C.  $2\theta_{\text{max}}(\text{MoK}\alpha) = 50^\circ$ . Number of data measured, 2953. Number of unique data, 831. Number of data having  $F_o^2 > 3\sigma(F_o^2)$ , 326. Number of variables, 33. Number of atoms, 5.  $\mu = 502$  cm<sup>-1</sup>. Final  $R = 0.057$  and  $R_w = 0.063$ . (c) Crystal data for  $\text{K}_2\text{Hg}_3\text{Se}_4$ : orthorhombic  $Pbcn$ ,  $Z = 4$ ,  $a = 10.820$  (2) Å,  $b = 6.783$  (1) Å,  $c = 14.042$  (2) Å,  $V = 1030.6$  Å<sup>3</sup> at -120 °C.  $2\theta_{\text{max}}(\text{MoK}\alpha) = 50^\circ$ . Number of data measured, 1088. Number of unique data, 903. Number of data having  $F_o^2 > 3\sigma(F_o^2)$ , 567. Number of variables, 43. Number of atoms, 5.  $\mu = 593$  cm<sup>-1</sup>. Final  $R = 0.077$  and  $R_w = 0.084$ . An empirical absorption correction based on  $\psi$ -scans for several reflections was applied to all data sets.

(16) *Atlas of Zeolite Structure Types*; Meier, W. M., Olson, D. H., Eds.; Butterworths: London, 1988.

(17) A full account of this complex structure will be given elsewhere.

(18) Bonds and angles along with atomic labeling for this structure are given in the supplementary material.

structure types can be viewed as deriving from the successive dismantling of the three-dimensional adamantine structure of  $\text{HgS}^{19}$  as it attempts to accommodate the varying amounts of added  $\text{A}_2\text{Q}$ . For example the  $\mu_4$ -coordination of the  $\text{Q}^{2-}$  ions in the  $\text{HgQ}$  structure is reduced to  $\mu_3$ - and  $\mu_2$ -coordination in  $[\text{Hg}_6\text{Q}_7]_n^{2n-}$  and to only  $\mu_2$ -coordination in  $[\text{Hg}_3\text{Q}_4]_n^{2n-}$ . Another phase that also belongs to this homologous family is  $\text{K}_m\text{HgQ}_4^{20}$  ( $n = 3, m = 1$ ), which features discrete tetrahedral  $[\text{HgQ}_4]^{6-}$  units (the  $\text{HgQ}$  lattice has been reduced to individual  $[\text{HgQ}_4]^{6-}$  units). This is very similar to the successive breakup of the structures of the main-group elements (e.g., Si, P) that ensues upon reduction with very electropositive metals to form the familiar Zintl phases.<sup>21</sup>

The results reported here show that the three-dimensional structure of  $\text{HgQ}$  is tractable and can accommodate various amounts of alkali-metal monosulfides. It is likely that the  $\text{A}_2\text{Q}/\text{HgQ}$  system constitutes an infinitely adaptive pair similar to the  $(\text{ZnS})_n(\text{In}_2\text{S}_3)_m^{22}$  and  $(\text{BaS})_n(\text{FeS})_m^{23}$

systems. Work to identify other members of this family is continuing. In conclusion, using alkali-metal polychalcogenides as solvents and reagents is a viable synthetic and crystal growth route to novel chalcogenide solid-state materials.

**Acknowledgment.** Financial support from the Center for Fundamental Materials Research (CFMR) Michigan State University and the National Science Foundation for a Presidential Young Investigator Award, CHE-8958451, is gratefully acknowledged.

**Supplementary Material Available:** Tables of atomic coordinates of all atoms and anisotropic and isotropic thermal parameters of all non-hydrogen atoms, bond distances and angles, and a figure with the atomic labeling of  $\text{K}_2\text{Hg}_6\text{S}_7$  (7 pages); a listing of calculated and observed ( $10F_o/10F_c$ ) structure factors (14 pages). Ordering information is given on any current masthead page.

- (19) Toshikazu, O. *J. Appl. Crystallogr.* 1974, 7, 396-397.  
 (20) Sommer, H.; Hoppe, R. Z. *Anorg. Allg. Chem.* 1978, 443, 201-211.  
 (21) (a) von Schnering, H.-G.; Nönle, W. *Chem. Rev.* 1988, 88, 243-273.  
 (b) von Schnering, H.-G. *Angew. Chem., Int. Ed. Engl.* 1981, 20, 33-51.  
 (c) Schafer, H. *Ann. Rev. Mater. Sci.* 1985, 15, 1-41.

- (22) (a) Donika, F. G.; Kiosse, G. A.; Radautsan, S. I.; Semiletov, S. A.; Zhitar, V. F. *Sov. Phys. Crystallogr.* 1968, 12, 745-749. (b) Boorman, R. S.; Sutherland, J. K. *J. Mater. Sci.* 1969, 4(8), 658-671. (c) Barnett, D. E.; Boorman, R. S.; Sutherland, J. K. *Phys. Status Solidi A* 1971, 4(1), K49-K52.

- (23) (a) Grey, I. E. *J. Solid State Chem.* 1974, 11, 128-134. (b) Cohen, S.; Rendon-DiazMiron, L. E.; Steinfink, H. *J. Solid State Chem.* 1978, 25, 179-187. (c) Hoggins, J. T.; Steinfink, H. *Acta Crystallogr., Sect. B* 1977, 33, 673-678.

## Articles

### Reactivity of Metal Oxides $\text{Cu}_2\text{O}$ , $\text{MnO}$ , $\text{CoO}$ , $\text{NiO}$ , $\text{CuO}$ , and $\text{ZnO}$ with Indialite

G. Pourroy,\* J. L. Guille, and P. Poix

*I.P.C.M.S. Groupe de Chimie des Matériaux Inorganiques UM 380046 E.H.I.C.S.,  
1 rue Blaise Pascal BP 296, 67008 Strasbourg Cedex, France*

Received May 24, 1989

Reactivities of  $\text{Cu}_2\text{O}$ ,  $\text{MnO}$ ,  $\text{CoO}$ ,  $\text{NiO}$ ,  $\text{CuO}$ , and  $\text{ZnO}$  with indialite ( $\text{Mg}_2\text{Al}_4\text{Si}_5\text{O}_{18}$ ) are studied under air, argon, or vacuum and for temperatures between 800 and 1150 °C, by using X-ray diffraction, magnetic measurements, and ESR spectroscopy. While  $\text{Cu}_2\text{O}$  is inert toward indialite, MO oxides always react: small quantities of cupric oxide disappear in indialite phase at about 950-1000 °C under air and appear again partly above 1030 °C. Magnetic measurements and ESR spectroscopy prove that the oxidation degree of dissolved copper is 2+ and that this dissolved copper does not behave as copper in cupric oxide. For greater concentrations of  $\text{CuO}$ , a spinel phase appears. The other MO oxides always destroy the indialite framework, giving  $\text{M}_2\text{SiO}_4$  and a spinel phase for manganese, cobalt, and nickel oxides,  $\alpha\text{-SiO}_2$ ,  $\text{MgSiO}_3$ , and  $\text{ZnAl}_2\text{O}_4$  in the zinc case.

#### Introduction

Until now, cordierite ( $\text{Mg}_2\text{Al}_4\text{Si}_5\text{O}_{18}$ ) has given rise to a rich literature because of its unusual physical properties. Its relatively low polycrystalline linear thermal expansion  $\alpha_p$  ( $1 \times 10^{-6}$ - $4 \times 10^{-6}/^\circ\text{C}$ ), low dielectric constant (4-6), and high volume resistivity ( $>10^4 \Omega \text{ cm}$ ) make it attractive for catalyst carriers and application in electronic packaging.

$\text{Mg}$  cordierite exists under three polymorphic forms: a hexagonal high-temperature form, named indialite or  $\alpha$ -cordierite, isostructural with beryl (space group  $P6/mmc$ ), an orthorhombic low-temperature form designed  $\beta$ -cordierite (space group  $Cccm$ ) which is the most encountered

structure for natural cordierite, and a metastable form,  $\mu$ -cordierite.<sup>1-3</sup> The hexagonal and orthorhombic structures are characterized by their six-membered rings of tetrahedrally coordinated cations ( $\text{T}_2$ ) perpendicular to the  $c$  axis. Alternate layers of the hexagonal ring structure are connected through  $\text{Mg}$  octahedra and  $\text{T}_1$  tetrahedra (Figure 1). Silicon occupies mostly  $\text{T}_2$  tetrahedra, and aluminum  $\text{T}_1$  tetrahedra. Differences between high- and

(1) Karkhanavala, M. D.; Hummell, F. A. *J. Am. Ceram. Soc.* 1953, 36(12), 389-92.

(2) Gibbs, G. V. *Am. Mineral.* 1966, 51, 1068-87.

(3) Meagher, E. P.; Gibbs, G. V. *Can. Mineral.* 1977, 15, 43-49.